Beam energy dependence of the linear and mode-coupled flow harmonics in Au+Au collisions

The STAR Collaboration

Abstract

The linear and mode-coupled contributions to higher-order anisotropic flow are presented for Au+Au collisions at $\sqrt{s_{NN}}$ = 27, 39, 54.4, and 200 GeV and compared to similar measurements for Pb+Pb collisions at the Large Hadron Collider (LHC). The coefficients and the flow harmonics' correlations, which characterize the linear and mode-coupled response to the lower-order anisotropies, indicate a beam energy dependence consistent with an influence from the specific shear viscosity (η/s). In contrast, the dimensionless coefficients, mode-coupled response coefficients, and normalized symmetric cumulants are approximately beam-energy independent, consistent with a significant role from initial-state effects. These measurements could provide unique supplemental constraints to (i) distinguish between different initial-state models and (ii) delineate the temperature (T) and baryon chemical potential (μ_B) dependence of the specific shear viscosity $\frac{\eta}{s}(T, \mu_B)$.

Keywords: Collectivity, correlation, shear viscosity
PACS: 25.75.-Ld

arXiv:2211.11637v1 [nucl-ex] 21 Nov 2022

Experimental studies of heavy-ion collisions at the LHC and the Relativistic Heavy Ion Collider (RHIC) indicate the creation of the Quark-Gluon Plasma (QGP) [1–4], a state of matter implied by Quantum Chromodynamics (QCD). A central aim of prior and current experimental investigations of this plasma is to understand its transport properties such as its specific viscosity or ratio of shear viscosity to entropy density (η/s) [5–11]. Anisotropic flow measurements continue to be a valuable route to η/s estimation because they reflect the viscous hydrodynamic response to the anisotropy of the initial-state energy density [6, 12–24] which is characterized by the complex eccentricity vectors $\mathcal{E}_n$ [25–29]:

$$\mathcal{E}_n \equiv \varepsilon_n e^{in\Phi_n} \equiv -\frac{\int dx^{'}\, dy^{'}\, r^n\, e^{in\phi}\, \rho_e(r,\phi)}{\int dx^{'}\, dy^{'}\, r^n\, \rho_e(r,\phi)},\ (n > 1), \tag{1}$$

where ε_n and Φ_n are the magnitude and azimuthal direction of the $\mathrm{n^{th}}$ eccentricity vector, $x^{'} = r\ \cos\phi$, $y^{'} = r\ \sin\phi$, r is the radial coordinate, ϕ is the spatial azimuthal angle, and $\rho_e(r,\phi)$ is the initial energy density profile [28, 30, 31].

The azimuthal anisotropy of particles produced relative to the reaction plane can be expressed as [32]:

$$E_p \frac{d^3N}{d^3p} = \frac{1}{2\pi}\frac{d^2N}{p_T dp_T dy}\left(1 + \sum_{i=1}^{N} 2v_n \cos\left(n\left(\varphi - \psi_n\right)\right)\right), \tag{2}$$

where N is the number of the particles produced, E_p is the energy of the particle, v_n is the n^{th} order flow coefficient, p_T is transverse momentum, y is the rapidity, φ is the azimuthal angle of the particle's momentum, and ψ_n is the n^{th}-order symmetry plane. The coefficients v_1, v_2, and v_3 are commonly termed directed, elliptic and triangular flow, respectively.

Prior investigations of v_2 and v_3 and their fluctuations [29, 33–44] as well as higher-order flow harmonics v_n ($n > 3$) [20, 35, 39, 45–50] have provided invaluable initial insights into the properties of the QGP. Notably, the extensively studied v_2 [39, 51–53] and v_3 flow coefficients [46, 54] are linearly related to ε_2 and ε_3 [17, 29, 55–62]:

$$v_n = \kappa_n \varepsilon_n, \tag{3}$$

where the parameter κ_n encodes the effects of viscous attenuation [46, 61, 63] which depend on the particle p_T, charged particle multiplicity and η/s . The higher-order flow harmonics show a linear response to the same-order eccentricity but also include a mode-coupled response to the lower-order eccentricities ε_2 and ε_3 [22, 30, 31, 64]:

$$\begin{aligned} V_4 &= v_4 e^{i4\psi_4} = \kappa_4\varepsilon_4 e^{4i\Phi_4} + \kappa_4^{'}\varepsilon_2^2 e^{4i\Phi_2} \\ &= V_4^{\mathrm{Linear}} + \chi_{4,22} V_4^{\mathrm{MC}}, \end{aligned} \tag{4}$$

$$\begin{aligned} V_5 &= v_5 e^{i5\psi_5} = \kappa_5\varepsilon_5 e^{5i\Phi_5} + \kappa_5^{'}\varepsilon_2 e^{2i\Phi_2}\varepsilon_3 e^{3i\Phi_3} \\ &= V_5^{\mathrm{Linear}} + \chi_{5,23} V_5^{\mathrm{MC}}, \end{aligned} \tag{5}$$

where $\kappa_k^{'}$ ($k = 4, 5$) reflects the combined influence of the medium properties and the coupling between the lower- and higher-order eccentricity harmonics. In Eqs. (4) and (5) the terms V_k^{Linear} and V_k^{MC} are the linear and the mode-coupled contributions and $\chi_{k,nm}$ represents the mode-coupled response coefficients. The normalized symmetric cumulants (NSC(n, m)) [65, 66] are also expected to give a measure of the mode-coupled contributions.

The mode-coupled contributions to V_k and $\mathrm{NSC(n,m)}$ can provide further constraints for η/s and the initial-stage dynamics [30, 33, 34, 38, 66–71]. Consequently, ongoing efforts seek to leverage extensive measurements of the linear and mode-coupled contributions to V_k and $\mathrm{NSC(n,m)}$ to develop unique supplemental constraints that can (i) distinguish between different initial-state models and (ii) pin down the temperature (T) and baryon chemical potential (μ_B) dependence of the specific shear viscosity $\frac{\eta}{s}(T,\mu_B)$. Prior measurements have been reported for charged hadrons in Pb+Pb collisions at $\sqrt{s_{NN}} = 2.76$ and 5.02 TeV [72–74] and Au+Au collisions at $\sqrt{s_{NN}} = 200$ GeV [11, 33], and for identified particle species in Pb+Pb collisions at $\sqrt{s_{NN}} = 2.76$ GeV [72]. Here, we report the V_n^{Linear}, V_n^{MC}, $\chi_{k,nm}$ and $\mathrm{NSC(n,m)}$ measurements for Au+Au collisions at $\sqrt{s_{NN}} = 27$, 39, 54.4, and 200 GeV to extend the data set that can provide simultaneous constraints for $\frac{\eta}{s}(T,\mu_B)$ and the initial-state. The initial-state effects which influence the dimensionless mode-coupled coefficients and the normalized symmetric cumulants could be insensitive to the beam energy, while $\frac{\eta}{s}(T,\mu_B)$ is not [75–77].

The data for the present analysis were collected with the STAR detector at RHIC using a minimum-bias trigger [78] in 2017, 2010 and 2018 at $\sqrt{s_{NN}} = 54.4$, 39 and 27 GeV respectively. Charged particle tracks with full azimuthal angle and pseudorapidity $|\eta| < 1.0$ coverage were used to reconstruct the collision vertices of tracks measured in the Time Projection Chamber (TPC) [79]. A Monte Carlo Glauber simulation has been used to determine the collision centrality from the measured event-by-event charged particle multiplicity in $|\eta| < 0.5$ with at least 10 hits [80, 81]. In this analysis, tracks with at least 15 TPC space points and Distance of Closest Approach (DCA) to the primary vertex of less than 3 cm were used. We accept tracks with transverse momentum $0.2 < p_{\mathrm{T}} < 4$ GeV/c. Events are chosen with vertex positions within ± 40 cm from the TPC center (along the beam direction), and within ± 2 cm in the radial direction relative to the center of the TPC.

The two- and multi-particle cumulant methods are employed for our correlation analysis. The framework for the cumulant method is described in Refs. [65, 66]; its extension to the case of subevents is also described in Refs. [82, 83]. Here, the two- and multi-particle correlations were formed using the two-subevents cumulant technique [83], with $\Delta\eta = \eta_1 - \eta_2 > 0.7$ between the subevents A and B (*i.e.*, $\eta_A > 0.35$ and $\eta_B < -0.35$). The use of the two-subevents technique serves to reduce the nonflow correlations [84]. The two- and multi-particle correlations are given as:

$$v_k^{\mathrm{Inclusive}} = \langle\langle\cos(k(\varphi_1^A - \varphi_2^B))\rangle\rangle^{1/2}, \quad (6)$$

$$C_{k,nm} = \langle\langle\cos(k\varphi_1^A - n\varphi_2^B - m\varphi_3^B)\rangle\rangle, \quad (7)$$

$$\langle v_n^2 v_m^2\rangle = \langle\langle\cos(n\varphi_1^A + m\varphi_2^A - n\varphi_3^B - m\varphi_4^B)\rangle\rangle \quad (8)$$

where $\langle\langle\,\rangle\rangle$ denotes the average over all particles in a single event and a subsequent average over all events, $k = n+m$, $n = 2$, $m = 2$ or 3, and φ_i is the azimuthal angle of the momentum of the i^{th} particle.

Using Eqs. (6)-(8), the mode-coupled contributions to v_k, assuming factorization, can be expressed as [31, 85]:

$$\begin{aligned} v_k^{\mathrm{MC}} &= \frac{C_{k,nm}}{\sqrt{\langle v_n^2 v_m^2\rangle}}, \\ &\sim \langle v_k \cos(k\Psi_k - n\Psi_n - m\Psi_m)\rangle, \end{aligned} \quad (9)$$

and the linear contribution to v_k is given by:

$$v_k^{\mathrm{Linear}} = \sqrt{(v_k^{\mathrm{Inclusive}})^2 - (v_k^{\mathrm{MC}})^2}. \quad (10)$$

Equation (10) assumes that the linear and mode-coupled contributions to v_k are independent [31, 84]. The ratio of the mode-coupled contribution to the inclusive v_k also gives an estimate of the correlation $\rho_{k,nm}$ between flow symmetry planes of order n and m[72];

$$\begin{aligned} \rho_{k,nm} &= \frac{v_k^{\mathrm{MC}}}{v_k^{\mathrm{Inclusive}}}, \\ &\approx \langle\cos(k\Psi_k - n\Psi_n - m\Psi_m)\rangle. \end{aligned} \quad (11)$$

The mode-coupled response coefficients, $\chi_{k,nm}$, which quantify the contributions of the coupling to the the higher-order anisotropic flow harmonics, are defined as:

$$\chi_{k,nm} = \frac{v_k^{\mathrm{MC}}}{\sqrt{\langle v_n^2\, v_m^2\rangle}}. \quad (12)$$

The normalized symmetric cumulants, $\mathrm{NSC(n,m)}$, from the standard cumulants method [65, 66] are given as:

$$\begin{aligned} \mathrm{SC(n,m)} &= \langle\langle\cos(n\varphi_1 + m\varphi_2 - n\varphi_3 - m\varphi_4)\rangle\rangle \\ &- \langle\langle\cos(n(\varphi_1 - \varphi_2))\rangle\rangle \\ &\quad \langle\langle\cos(m(\varphi_1 - \varphi_2))\rangle\rangle \end{aligned} \quad (13)$$

$$\mathrm{NSC(n,m)} = \frac{\mathrm{SC(n,m)}}{(v_n^{\mathrm{Inclusive}})^2\,(v_m^{\mathrm{Inclusive}})^2}, \quad (14)$$

with the condition that $m \neq n$ and n and m are positive integers. The p_T-integrated measurements for $k = n+m$, $n = 2$, $m = 2$ and 3 were performed as a function of centrality for each beam energy.

The systematic uncertainties of the presented measurements are obtained from variations in the analysis cuts for event selection, track selection and non-flow suppression; (I) event selection was varied via cuts on the vertex positions determined in the TPC along the beam direction, -40 to 0 cm or 0 to 40 cm instead of the nominal value of ± 40 cm. (II) Track selection was varied by (a) reducing the DCA from its nominal value of 3 cm to 2 cm, and (b) increasing the number of TPC space points from greater than 15 points to more than 20 points. (III) The pseudorapidity gap, $\Delta\eta$ for the track pairs, used to mitigate the non-flow effects due to resonance decays, Bose-Einstein correlations, and the fragments of individual jets, was varied from $\Delta\eta = 0.6$ to $\Delta\eta = 0.8$. Table 1 gives a sum-

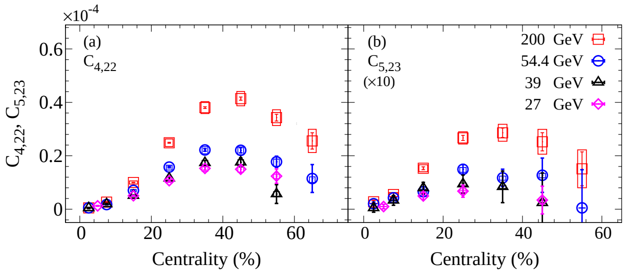

Figure 1: Comparison of the p_{T} integrated three-particle correlators, $C_{4,22}$ (a) and $C_{5,23}$ (b), for Au+Au collisions at $\sqrt{s_{NN}}$ = 54.4, 39 and 27 GeV, obtained with the two-subevents cumulant method. The $C_{4,22}$ and $C_{5,23}$ measurements for Au+Au at $\sqrt{s_{NN}}$ = 200 GeV are taken from Ref. [11].

mary of these systematic uncertainty estimates. The overall systematic uncertainty, assuming independent sources, was evaluated via a quadrature sum of the uncertainties resulting from the respective cut variations. They range from 4% to 10% from central to peripheral collisions. The overall systematic uncertainties are shown as open boxes in the figures. Statistical uncertainties are shown as vertical lines.

Quantities	Minimum value	Maximum value
Event	2%	5%
Track	3%	7%
$\Delta\eta$	2%	7%

Table 1: Summary of the estimated systematic uncertainty contributions (see text).

Figure 1 compares the centrality dependence of the $C_{4,22}$ and $C_{5,23}$ coefficients for $0.2 < p_{\mathrm{T}} < 4.0$ GeV/c in Au+Au collisions at $\sqrt{s_{NN}}$ = 200, 54.4, 39 and 27 GeV. The coefficients show similar centrality-dependent patterns and magnitudes that decrease with beam energy. These dependencies suggests that $C_{4,22}$ and $C_{5,23}$ are sensitive to the initial-state eccentricity and the change in viscous attenuation with beam energy. The latter could result from both a change in the charge particle multiplicity and $\eta/s(\mu_B, T)$ [75, 76] with beam energy. Thus, detailed model comparisons to the centrality and beam energy dependence of $C_{4,22}$ and $C_{5,23}$ could serve as an additional constraint for precision extraction of η/s [77].

The $v_k^{\mathrm{Inclusive}}$, $C_{4,22}$ and $C_{5,23}$ coefficients were used to extract v_k^{MC}, v_k^{Linear}, $\rho_{k,nm}$, $\chi_{k,nm}$, and NSC(n, m) (cf. Eqs. 9 − 14) to home in on further constraints for the initial- and final-states respectively. The centrality dependence of $v_k^{\mathrm{Inclusive}}$ ((a) and (d)), v_k^{Linear} ((b) and (e)), and v_k^{MC} ((c) and (f)) $v_{4,5}$ coefficients are shown for several beam energies in Fig. 2. The mode-coupled coefficients ((b) and (e)) indicate a much stronger increase with centrality than that for the linear coefficients ((c) and (f)), suggesting that the v_k^{Linear} coefficients are subject to much larger viscous attenuation than the v_k^{MC} coefficients; note that $\varepsilon_k^{\mathrm{MC}}$ and $\varepsilon_k^{\mathrm{Linear}}$ increase with centrality. The v_k^{MC} and v_k^{Linear} coefficients for Au+Au collisions also indicate a relatively weak dependence on beam energy, suggesting that the viscous attenuation and the eccentricity are weak functions of the beam energy (cf. Eq. 3) especially for the energy span $\sqrt{s_{NN}}$ = 27 - 54.4 GeV. The LHC measurements (set-1 [72], for $0.2 < p_{\mathrm{T}} < 5.0$ GeV/c and $|\eta| < 0.8$, and set-2 [38], for $p_{\mathrm{T}} > 0.5$ GeV/c and $|\eta| < 2.5$) (panels (a)–(f)) show patterns that are similar to those for Au+Au collisions, albeit with magnitudes that are much larger, implying a more sizable dependence on beam energy from RHIC to LHC energies [75, 77]. The difference between the magnitudes for the set-1 and set-2 LHC measurements reflects the dependence of these coefficients on $\langle p_T \rangle$. Ref. [11] has reported a qualitatively similar dependence at lower beam energy. Note however, that the $\langle p_T \rangle$ is a weak function of the RHIC beam energy range of interest in this work [86]. These beam energy and centrality dependencies can be used to further constrain theoretical models.

The centrality dependence of the mode-coupled response coefficients $\chi_{k,nm}$ ($n = 2$ and $m = 2$ and 3) for Au+Au ($\sqrt{s_{NN}}$ = 200, 54.4, 39 and 27 GeV) and Pb+Pb collisions ($\sqrt{s_{NN}}$ = 2.76 TeV) [72] are compared in Figs. 3 (a) and (b). Results demonstrate a weak dependence on centrality and beam energy, confirming that (I) the mode-coupled $v_{4,5}$ coefficients are dominated by the correlations from the lower-order flow harmonics and (II) $\chi_{k,nm}$ is weakly sensitive to the viscous effects (η/s) [75, 77] and hence, more sensitive to the initial-state effects.

Figure 3 (c) and (d) compares the centrality dependence of the $\rho_{k,nm}$ coefficients for Au+Au collisions ($\sqrt{s_{NN}}$ = 200, 54.4, 39 and 27 GeV) and Pb+Pb collisions ($\sqrt{s_{NN}}$ = 2.76 TeV) [72]. They indicate a strong centrality dependence and a relatively weak dependence on beam energy. These characteristic dependencies suggests that $\rho_{k,nm}$ can provide a supplemental constraint for the beam energy dependence of the viscous effects (η/s) [75, 77] and could be used to discern different initial-state models [77].

Figure 4 summarizes the results for the NSC(n, m) that reflect the strength of the correlation/anti-correlation between the v_n and v_m flow harmonics. Figs. 4(a) and (b) show the NSC(2, 3) and NSC(2, 4) respectively, for $0.2 < p_{\mathrm{T}} < 4.0$ GeV/c in Au+Au collisions at $\sqrt{s_{NN}}$ = 200, 54.4 and 27 GeV and the corresponding LHC measurements [34]. The NSC(2, 3) coefficients indicate an anti-correlation (negative values) [67, 87] between v_2 and v_3, as expected from the known anti-correlation between ε_2 and ε_3. In contrast, the NSC(2, 4) coefficients indicate a correlation between v_2 and v_4 consistent with the mode-coupled correlations between ε_2 and ε_4. The weak beam energy dependence further indicates that NSC(2, 3) and NSC(2, 4) are insensitive to the effects of viscous attenuation [75] and could set a constraint on the initial-state eccentricity correlations.

In summary, we have presented new p_{T}-integrated measurements of the charge-inclusive, linear and mode-coupled contributions to the higher-order anisotropic flow coefficients $v_{4,5}$, mode-coupled response coefficients $\chi_{k,nm}$, correlations of the event plane angles $\rho_{k,nm}$ and normalized

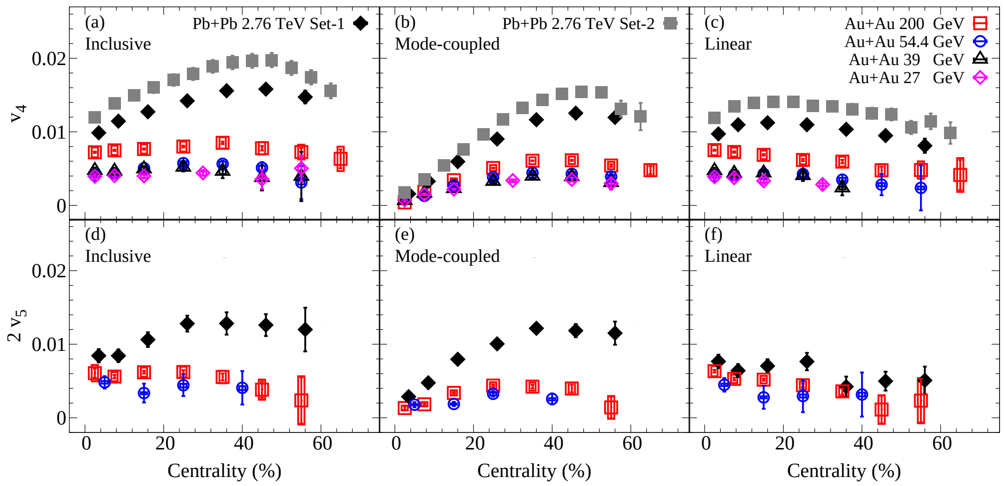

Figure 2: Comparison of the inclusive ((a) and (d)), mode-coupled ((b) and (e)) and linear ((c) and (f)) higher-order flow harmonics v_4 and v_5 obtained with the two-subevents cumulant method, as a function of centrality in the p_{T} range $0.2-4.0$ GeV/c for Au+Au collisions at $\sqrt{s_{NN}}$ = 54.4, 39 and 27 GeV. The v_4 and v_5 measurements of $\sqrt{s_{NN}}$ = 200 GeV are taken from Ref. [11]. The solid points indicate LHC measurements for p_{T} in the range $0.2-5.0$ GeV/c set-1 [72] and $p_{\mathrm{T}} > 0.5$ GeV/c set-2 [38] for Pb+Pb collisions at $\sqrt{s_{NN}}$ = 2.76 TeV.

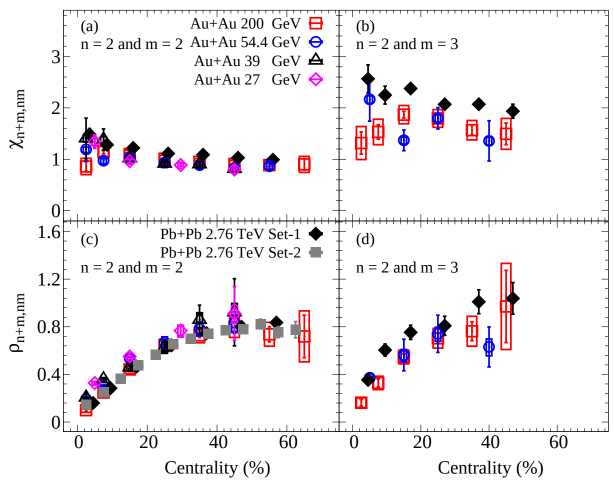

Figure 3: Comparison of the $\chi_{n+m,nm}$ ((a) and (c)) and $\rho_{n+m,nm}$ ((b) and (d)) obtained with the two-subevents cumulant method, as a function of centrality in the p_{T} range $0.2-4.0$ GeV/c for Au+Au collisions at $\sqrt{s_{NN}}$ = 54.4, 39 and 27 GeV. The $\chi_{n+m,nm}$ and $\rho_{n+m,nm}$ at $\sqrt{s_{NN}}$ = 200 GeV are taken from Ref. [11]. The solid points are the LHC measurements for Pb+Pb collisions at $\sqrt{s_{NN}}$ = 2.76 TeV set-1 [72] and set-2 [38].

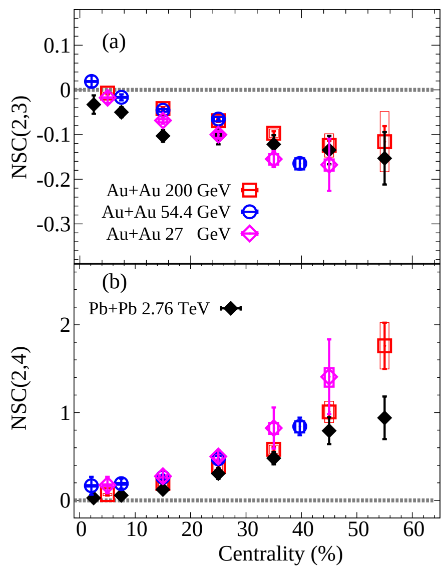

Figure 4: Comparison of NSC(2, 3) (a) and NSC(2, 4) (b) using the standard cumulant method as a function of centrality in the p_{T} range 0.2–4.0 GeV/c for Au+Au collisions at $\sqrt{s_{NN}}$ = 54.4, 39 and 27 GeV. The NSC(2, 3) and NSC(2, 4) at $\sqrt{s_{NN}}$ = 200 GeV are taken from Ref. [33]. The solid diamonds indicate LHC measurements for the p_{T} range from 0.2–5.0 GeV/c for Pb+Pb collisions at $\sqrt{s_{NN}}$ = 2.76 TeV [34].

symmetric cumulant NSC(2, 3) and NSC(2, 4), for Au+Au collisions at $\sqrt{s_{NN}}$ = 200, 54.4, 39 and 27 GeV. Our measurements are compared with similar LHC measurements for Pb+Pb collisions at $\sqrt{s_{NN}}$ = 2.76 TeV. For all presented energies, the mode-coupled $v_{4,5}$ measurements indicate a large centrality dependence. In contrast, the linear $v_{4,5}$, which dominates the central collisions, displays a weak centrality dependence. The $v_{4,5}$ measurements show a beam energy dependence which reflects the sensitivity to η/s. The dimensionless coefficients $\chi_{k,nm}$, $\rho_{k,nm}$, NSC(2, 3) and NSC(2, 4) show magnitudes and trends which are approximately beam energy independent, suggesting that the measured dimensionless quantities are dominated by initial-state effects. These results should prove invaluable to theoretical efforts which seek simultaneous constraints for $\frac{\eta}{s}(T, \mu_B)$ and the initial-state.

Acknowledgments

We thank the RHIC Operations Group and RCF at BNL, the NERSC Center at LBNL, and the Open Science Grid consortium for providing resources and support. This work was supported in part by the Office of Nuclear Physics within the U.S. DOE Office of Science, the U.S. National Science Foundation, National Natural Science Foundation of China, Chinese Academy of Science, the

Ministry of Science and Technology of China and the Chinese Ministry of Education, the Higher Education Sprout Project by Ministry of Education at NCKU, the National Research Foundation of Korea, Czech Science Foundation and Ministry of Education, Youth and Sports of the Czech Republic, Hungarian National Research, Development and Innovation Office, New National Excellency Programme of the Hungarian Ministry of Human Capacities, Department of Atomic Energy and Department of Science and Technology of the Government of India, the National Science Centre of Poland, the Ministry of Science, Education and Sports of the Republic of Croatia, German Bundesministerium für Bildung, Wissenschaft, Forschung and Technologie (BMBF), Helmholtz Association, Ministry of Education, Culture, Sports, Science, and Technology (MEXT) and Japan Society for the Promotion of Science (JSPS).

References

[1] E. V. Shuryak, Quark-Gluon Plasma and Hadronic Production of Leptons, Photons and Psions, Phys. Lett. B 78 (1978) 150. doi:10.1016/0370-2693(78)90370-2.

[2] E. V. Shuryak, Quantum Chromodynamics and the Theory of Superdense Matter, Phys. Rept. 61 (1980) 71–158. doi:10.1016/0370-1573(80)90105-2.

[3] B. Muller, J. Schukraft, B. Wyslouch, First Results from Pb+Pb collisions at the LHC, Ann. Rev. Nucl. Part. Sci. 62 (2012) 361–386. doi:10.1146/annurev-nucl-102711-094910.

[4] K. H. Ackermann, et al., Elliptic flow in Au + Au collisions at (S(NN))**(1/2) = 130 GeV, Phys. Rev. Lett. 86 (2001) 402–407. arXiv:nucl-ex/0009011, doi:10.1103/PhysRevLett.86.402.

[5] E. Shuryak, Why does the quark gluon plasma at RHIC behave as a nearly ideal fluid?, Prog. Part. Nucl. Phys. 53 (2004) 273–303. doi:10.1016/j.ppnp.2004.02.025.

[6] P. Romatschke, U. Romatschke, Viscosity Information from Relativistic Nuclear Collisions: How Perfect is the Fluid Observed at RHIC?, Phys.Rev.Lett. 99 (2007) 172301. doi:10.1103/PhysRevLett.99.172301.

[7] M. Luzum, P. Romatschke, Conformal Relativistic Viscous Hydrodynamics: Applications to RHIC results at s(NN)**(1/2) = 200-GeV, Phys.Rev. C78 (2008) 034915. doi:10.1103/PhysRevC.78.034915.

[8] P. Bozek, Bulk and shear viscosities of matter created in relativistic heavy-ion collisions, Phys. Rev. C 81 (2010) 034909. doi:10.1103/PhysRevC.81.034909.

[9] S. Acharya, et al., Investigations of Anisotropic Flow Using Multiparticle Azimuthal Correlations in pp, p-Pb, Xe-Xe, and Pb-Pb Collisions at the LHC, Phys. Rev. Lett. 123 (14) (2019) 142301. doi:10.1103/PhysRevLett.123.142301.

[10] S. Acharya, et al., Higher harmonic non-linear flow modes of charged hadrons in Pb-Pb collisions at $\sqrt{s_{\rm NN}} = 5.02$ TeV, JHEP 05 (2020) 085. doi:10.1007/JHEP05(2020)085.

[11] J. Adam, et al., Investigation of the linear and mode-coupled flow harmonics in Au+Au collisions at $\sqrt{S_{NN}} = 200$ GeV, Phys. Lett. B809 (2020) 135728. doi:10.1016/j.physletb.2020.135728.

[12] U. W. Heinz, P. F. Kolb, Early thermalization at RHIC, Nucl. Phys. A702 (2002) 269–280. doi:10.1016/S0375-9474(02)00714-5.

[13] T. Hirano, U. W. Heinz, D. Kharzeev, R. Lacey, Y. Nara, Hadronic dissipative effects on elliptic flow in ultrarelativistic heavy-ion collisions, Phys.Lett. B636 (2006) 299–304. doi:10.1016/j.physletb.2006.03.060.

[14] P. Huovinen, P. F. Kolb, U. W. Heinz, P. V. Ruuskanen, S. A. Voloshin, Radial and elliptic flow at RHIC: Further predictions, Phys. Lett. B503 (2001) 58–64. doi:10.1016/S0370-2693(01)00219-2.

[15] T. Hirano, K. Tsuda, Collective flow and two pion correlations from a relativistic hydrodynamic model with early chemical freeze out, Phys. Rev. C66 (2002) 054905. doi:10.1103/PhysRevC.66.054905.

[16] M. Luzum, Flow fluctuations and long-range correlations: elliptic flow and beyond, J. Phys. G38 (2011) 124026. doi:10.1088/0954-3899/38/12/124026.

[17] H. Song, S. A. Bass, U. Heinz, T. Hirano, C. Shen, 200 A GeV Au+Au collisions serve a nearly perfect quark-gluon liquid, Phys. Rev. Lett. 106 (2011) 192301, [Erratum: Phys. Rev. Lett.109,139904(2012)]. doi:10.1103/PhysRevLett.106.192301.

[18] J. Qian, U. W. Heinz, J. Liu, Mode-coupling effects in anisotropic flow in heavy-ion collisions, Phys. Rev. C93 (6) (2016) 064901. doi:10.1103/PhysRevC.93.064901.

[19] N. Magdy (For the STAR Collaboration), Beam energy dependence of the anisotropic flow coefficients v_n, PoS CPOD2017 (2018) 005.

[20] N. Magdy (For the STAR Collaboration), Viscous Damping of Anisotropic Flow in 7.7 - 200 GeV Au+Au Collisions, J. Phys. Conf. Ser. 779 (1) (2017) 012060. doi:10.1088/1742-6596/779/1/012060.

[21] B. Schenke, S. Jeon, C. Gale, Anisotropic flow in $\sqrt{s} = 2.76$ TeV Pb+Pb collisions at the LHC, Phys.Lett. B702 (2011) 59–63. doi:10.1016/j.physletb.2011.06.065.

[22] D. Teaney, L. Yan, Non linearities in the harmonic spectrum of heavy ion collisions with ideal and viscous hydrodynamics, Phys. Rev. C86 (2012) 044908. doi:10.1103/PhysRevC.86.044908.

[23] F. G. Gardim, F. Grassi, M. Luzum, J.-Y. Ollitrault, Anisotropic flow in event-by-event ideal hydrodynamic simulations of $\sqrt{s_{NN}} = 200$ GeV Au+Au collisions, Phys.Rev.Lett. 109 (2012) 202302. doi:10.1103/PhysRevLett.109.202302.

[24] R. A. Lacey, D. Reynolds, A. Taranenko, N. N. Ajitanand, J. M. Alexander, F.-H. Liu, Y. Gu, A. Mwai, Acoustic scaling of anisotropic flow in shape-engineered events: implications for extraction of the specific shear viscosity of the quark gluon plasma, J. Phys. G43 (10) (2016) 10LT01. doi:10.1088/0954-3899/43/10/10LT01.

[25] B. H. Alver, C. Gombeaud, M. Luzum, J.-Y. Ollitrault, Triangular flow in hydrodynamics and transport theory, Phys. Rev. C82 (2010) 034913. doi:10.1103/PhysRevC.82.034913.

[26] H. Petersen, G.-Y. Qin, S. A. Bass, B. Muller, Triangular flow in event-by-event ideal hydrodynamics in Au+Au collisions at $\sqrt{s_{\rm NN}} = 200A$ GeV, Phys. Rev. C82 (2010) 041901. doi:10.1103/PhysRevC.82.041901.

[27] R. A. Lacey, R. Wei, N. N. Ajitanand, A. Taranenko, Initial eccentricity fluctuations and their relation to higher-order flow harmonics, Phys. Rev. C83 (2011) 044902. doi:10.1103/PhysRevC.83.044902.

[28] D. Teaney, L. Yan, Triangularity and Dipole Asymmetry in Heavy Ion Collisions, Phys. Rev. C83 (2011) 064904. doi:10.1103/PhysRevC.83.064904.

[29] Z. Qiu, U. W. Heinz, Event-by-event shape and flow fluctuations of relativistic heavy-ion collision fireballs, Phys. Rev. C84 (2011) 024911. doi:10.1103/PhysRevC.84.024911.

[30] R. S. Bhalerao, J.-Y. Ollitrault, S. Pal, Characterizing flow fluctuations with moments, Phys. Lett. B742 (2015) 94–98. doi:10.1016/j.physletb.2015.01.019.

[31] L. Yan, J.-Y. Ollitrault, $\nu_4, \nu_5, \nu_6, \nu_7$: nonlinear hydrodynamic response versus LHC data, Phys. Lett. B744 (2015) 82–87. doi:10.1016/j.physletb.2015.03.040.

[32] A. M. Poskanzer, S. A. Voloshin, Methods for analyzing anisotropic flow in relativistic nuclear collisions, Phys. Rev. C58 (1998) 1671–1678. doi:10.1103/PhysRevC.58.1671.

[33] J. Adam, et al., Correlation Measurements Between Flow Harmonics in Au+Au Collisions at RHIC, Phys. Lett. B783 (2018) 459–465. doi:10.1016/j.physletb.2018.05.076.

[34] J. Adam, et al., Correlated event-by-event fluctuations of flow harmonics in Pb-Pb collisions at $\sqrt{s_{\rm NN}} = 2.76$ TeV, Phys. Rev. Lett. 117 (2016) 182301.

doi:10.1103/PhysRevLett.117.182301.
[35] L. Adamczyk, et al., Harmonic decomposition of three-particle azimuthal correlations at energies available at the BNL Relativistic Heavy Ion Collider, Phys. Rev. C98 (3) (2018) 034918. doi:10.1103/PhysRevC.98.034918.
[36] A. Adare, et al., Measurements of Higher-Order Flow Harmonics in Au+Au Collisions at $\sqrt{s_{NN}} = 200$ GeV, Phys. Rev. Lett. 107 (2011) 252301. doi:10.1103/PhysRevLett.107.252301.
[37] G. Aad, et al., Measurement of event-plane correlations in $\sqrt{s_{NN}} = 2.76$ TeV lead-lead collisions with the ATLAS detector, Phys. Rev. C90 (2) (2014) 024905. doi:10.1103/PhysRevC.90.024905.
[38] G. Aad, et al., Measurement of the correlation between flow harmonics of different order in lead-lead collisions at $\sqrt{s_{NN}}$=2.76 TeV with the ATLAS detector, Phys. Rev. C92 (3) (2015) 034903. doi:10.1103/PhysRevC.92.034903.
[39] N. Magdy (For the STAR Collaboration), Collision system and beam energy dependence of anisotropic flow fluctuations, Nucl. Phys. A982 (2019) 255–258. doi:10.1016/j.nuclphysa.2018.09.027.
[40] B. Alver, et al., Importance of correlations and fluctuations on the initial source eccentricity in high-energy nucleus-nucleus collisions, Phys. Rev. C77 (2008) 014906. doi:10.1103/PhysRevC.77.014906.
[41] B. Alver, et al., Non-flow correlations and elliptic flow fluctuations in gold-gold collisions at $\sqrt{s_{NN}} = 200$ GeV, Phys. Rev. C81 (2010) 034915. doi:10.1103/PhysRevC.81.034915.
[42] J.-Y. Ollitrault, A. M. Poskanzer, S. A. Voloshin, Effect of flow fluctuations and nonflow on elliptic flow methods, Phys. Rev. C80 (2009) 014904. doi:10.1103/PhysRevC.80.014904.
[43] N. Magdy, Measuring differential flow angle fluctuations in relativistic nuclear collisions, Phys. Rev. C 106 (4) (2022) 044911. arXiv:2207.04530, doi:10.1103/PhysRevC.106.044911.
[44] M. Abdallah, et al., Collision-system and beam-energy dependence of anisotropic flow fluctuations (1 2022). arXiv:2201.10365.
[45] N. Magdy (For the STAR Collaboration), Beam-energy dependence of the azimuthal anisotropic flow from RHIC (2019). arXiv:1909.09640.
[46] J. Adam, et al., Azimuthal Harmonics in Small and Large Collision Systems at RHIC Top Energies, Phys. Rev. Lett. 122 (17) (2019) 172301. doi:10.1103/PhysRevLett.122.172301.
[47] L. Adamczyk, et al., Azimuthal anisotropy in Cu+Au collisions at $\sqrt{s_{NN}} = 200$ GeV, Phys. Rev. C98 (1) (2018) 014915. doi:10.1103/PhysRevC.98.014915.
[48] B. Alver, G. Roland, Collision geometry fluctuations and triangular flow in heavy-ion collisions, Phys. Rev. C81 (2010) 054905, [Erratum: Phys. Rev.C82,039903(2010)]. doi:10.1103/PhysRevC.82.039903,10.1103/PhysRevC.81.054905.
[49] S. Chatrchyan, et al., Measurement of higher-order harmonic azimuthal anisotropy in PbPb collisions at $\sqrt{s_{NN}} = 2.76$ TeV, Phys. Rev. C89 (4) (2014) 044906. doi:10.1103/PhysRevC.89.044906.
[50] N. Magdy, Impact of nuclear deformation on collective flow observables in relativistic U+U collisions (6 2022). arXiv:2206.05332.
[51] L. Adamczyk, et al., Measurement of elliptic flow of light nuclei at $\sqrt{s_{NN}} = 200$, 62.4, 39, 27, 19.6, 11.5, and 7.7 GeV at the BNL Relativistic Heavy Ion Collider, Phys. Rev. C 94 (3) (2016) 034908. doi:10.1103/PhysRevC.94.034908.
[52] L. Adamczyk, et al., Centrality dependence of identified particle elliptic flow in relativistic heavy ion collisions at $\sqrt{s_{NN}}$=7.7–62.4 GeV, Phys. Rev. C 93 (1) (2016) 014907. doi:10.1103/PhysRevC.93.014907.
[53] L. Adamczyk, et al., Azimuthal anisotropy in U+U and Au+Au collisions at RHIC, Phys. Rev. Lett. 115 (22) (2015) 222301. doi:10.1103/PhysRevLett.115.222301.
[54] L. Adamczyk, et al., Beam Energy Dependence of the Third Harmonic of Azimuthal Correlations in Au+Au Collisions at RHIC, Phys. Rev. Lett. 116 (11) (2016) 112302. doi:10.1103/PhysRevLett.116.112302.
[55] H. Niemi, G. S. Denicol, H. Holopainen, P. Huovinen, Event-by-event distributions of azimuthal asymmetries in ultrarelativistic heavy-ion collisions, Phys. Rev. C87 (5) (2013) 054901. doi:10.1103/PhysRevC.87.054901.
[56] F. G. Gardim, J. Noronha-Hostler, M. Luzum, F. Grassi, Effects of viscosity on the mapping of initial to final state in heavy ion collisions, Phys. Rev. C91 (3) (2015) 034902. doi:10.1103/PhysRevC.91.034902.
[57] J. Fu, Centrality dependence of mapping the hydrodynamic response to the initial geometry in heavy-ion collisions, Phys. Rev. C92 (2) (2015) 024904. doi:10.1103/PhysRevC.92.024904.
[58] H. Holopainen, H. Niemi, K. J. Eskola, Event-by-event hydrodynamics and elliptic flow from fluctuating initial state, Phys. Rev. C83 (2011) 034901. doi:10.1103/PhysRevC.83.034901.
[59] G.-Y. Qin, H. Petersen, S. A. Bass, B. Muller, Translation of collision geometry fluctuations into momentum anisotropies in relativistic heavy-ion collisions, Phys.Rev. C82 (2010) 064903. doi:10.1103/PhysRevC.82.064903.
[60] C. Gale, S. Jeon, B. Schenke, P. Tribedy, R. Venugopalan, Event-by-event anisotropic flow in heavy-ion collisions from combined Yang-Mills and viscous fluid dynamics, Phys. Rev. Lett. 110 (1) (2013) 012302. doi:10.1103/PhysRevLett.110.012302.
[61] P. Liu, R. A. Lacey, Acoustic scaling of linear and mode-coupled anisotropic flow; implications for precision extraction of the specific shear viscosity, Phys. Rev. C 98 (2) (2018) 021902. arXiv:1802.06595, doi:10.1103/PhysRevC.98.021902.
[62] N. Magdy, Characterizing the initial and final state effects of relativistic nuclear collisions (10 2022). arXiv:2210.14091.
[63] U. Heinz, R. Snellings, Collective flow and viscosity in relativistic heavy-ion collisions, Ann. Rev. Nucl. Part. Sci. 63 (2013) 123–151. doi:10.1146/annurev-nucl-102212-170540.
[64] F. G. Gardim, F. Grassi, M. Luzum, J.-Y. Ollitrault, Mapping the hydrodynamic response to the initial geometry in heavy-ion collisions, Phys. Rev. C 85 (2012) 024908. doi:10.1103/PhysRevC.85.024908.
[65] A. Bilandzic, R. Snellings, S. Voloshin, Flow analysis with cumulants: Direct calculations, Phys. Rev. C83 (2011) 044913. doi:10.1103/PhysRevC.83.044913.
[66] A. Bilandzic, C. H. Christensen, K. Gulbrandsen, A. Hansen, Y. Zhou, Generic framework for anisotropic flow analyses with multiparticle azimuthal correlations, Phys. Rev. C89 (6) (2014) 064904. doi:10.1103/PhysRevC.89.064904.
[67] Y. Zhou, Review of anisotropic flow correlations in ultrarelativistic heavy-ion collisions, Adv. High Energy Phys. 2016 (2016) 9365637. doi:10.1155/2016/9365637.
[68] Z. Qiu, U. Heinz, Hydrodynamic event-plane correlations in Pb+Pb collisions at $\sqrt{s} = 2.76$ATeV, Phys. Lett. B717 (2012) 261–265. doi:10.1016/j.physletb.2012.09.030.
[69] D. Teaney, L. Yan, Event-plane correlations and hydrodynamic simulations of heavy ion collisions, Phys. Rev. C90 (2) (2014) 024902. doi:10.1103/PhysRevC.90.024902.
[70] H. Niemi, K. J. Eskola, R. Paatelainen, Event-by-event fluctuations in a perturbative QCD + saturation + hydrodynamics model: Determining QCD matter shear viscosity in ultrarelativistic heavy-ion collisions, Phys. Rev. C93 (2) (2016) 024907. doi:10.1103/PhysRevC.93.024907.
[71] Y. Zhou, K. Xiao, Z. Feng, F. Liu, R. Snellings, Anisotropic distributions in a multiphase transport model, Phys. Rev. C93 (3) (2016) 034909. doi:10.1103/PhysRevC.93.034909.
[72] S. Acharya, et al., Linear and non-linear flow modes in Pb-Pb collisions at $\sqrt{s_{\rm NN}} = 2.76$ TeV, Phys. Lett. B773 (2017) 68–80. doi:10.1016/j.physletb.2017.07.060.
[73] S. Acharya, et al., Higher harmonic non-linear flow modes of charged hadrons in Pb-Pb collisions at $\sqrt{s_{\rm NN}} = 5.02$ TeV, JHEP 05 (2020) 085. doi:10.1007/JHEP05(2020)085.
[74] A. M. Sirunyan, et al., Mixed higher-order anisotropic flow and nonlinear response coefficients of charged particles in PbPb collisions at $\sqrt{s_{\rm NN}} = 2.76$ and 5.02 TeV, Eur. Phys. J. C 80 (6) (2020) 534. doi:10.1140/epjc/s10052-020-7834-9.
[75] R. A. Lacey, A. Taranenko, J. Jia, D. Reynolds, N. N. Aji-

tanand, J. M. Alexander, Y. Gu, A. Mwai, Beam energy dependence of the viscous damping of anisotropic flow in relativistic heavy ion collisions, Phys. Rev. Lett. 112 (8) (2014) 082302. doi:10.1103/PhysRevLett.112.082302.

[76] I. A. Karpenko, P. Huovinen, H. Petersen, M. Bleicher, Estimation of the shear viscosity at finite net-baryon density from $A+A$ collision data at $\sqrt{s_{\rm NN}} = 7.7 - 200$ GeV, Phys. Rev. C 91 (6) (2015) 064901. doi:10.1103/PhysRevC.91.064901.

[77] N. Magdy, Investigations of the linear and non-linear flow harmonics using the a multi-phase transport model, J. Phys. G 49 (1) (2022) 015105. arXiv:2106.09484, doi:10.1088/1361-6471/ac38c3.

[78] E. G. Judd, et al., The evolution of the STAR Trigger System, Nucl. Instrum. Meth. A902 (2018) 228–237. doi:10.1016/j.nima.2018.03.070.

[79] M. Anderson, et al., The Star time projection chamber: A Unique tool for studying high multiplicity events at RHIC, Nucl. Instrum. Meth. A499 (2003) 659–678. doi:10.1016/S0168-9002(02)01964-2.

[80] B. Alver, M. Baker, C. Loizides, P. Steinberg, The PHOBOS Glauber Monte Carlo (5 2008). arXiv:0805.4411.

[81] L. Adamczyk, et al., Inclusive charged hadron elliptic flow in Au + Au collisions at $\sqrt{s_{NN}} = 7.7$ - 39 GeV, Phys. Rev. C 86 (2012) 054908. arXiv:1206.5528, doi:10.1103/PhysRevC.86.054908.

[82] K. Gajdošová, Investigations of anisotropic collectivity using multi-particle correlations in pp, p–Pb and Pb–Pb collisions, Nucl. Phys. A967 (2017) 437–440. doi:10.1016/j.nuclphysa.2017.04.033.

[83] J. Jia, M. Zhou, A. Trzupek, Revealing long-range multiparticle collectivity in small collision systems via subevent cumulants, Phys. Rev. C96 (3) (2017) 034906. doi:10.1103/PhysRevC.96.034906.

[84] N. Magdy, O. Evdokimov, R. A. Lacey, A method to test the coupling strength of the linear and nonlinear contributions to higher-order flow harmonics via Event Shape Engineering, J. Phys. G 48 (2) (2020) 025101. doi:10.1088/1361-6471/abcb59.

[85] R. S. Bhalerao, J.-Y. Ollitrault, S. Pal, Event-plane correlators, Phys. Rev. C88 (2013) 024909. doi:10.1103/PhysRevC.88.024909.

[86] L. Adamczyk, et al., Bulk Properties of the Medium Produced in Relativistic Heavy-Ion Collisions from the Beam Energy Scan Program, Phys. Rev. C 96 (4) (2017) 044904. arXiv:1701.07065, doi:10.1103/PhysRevC.96.044904.

[87] G. Giacalone, L. Yan, J. Noronha-Hostler, J.-Y. Ollitrault, Symmetric cumulants and event-plane correlations in Pb + Pb collisions, Phys. Rev. C 94 (1) (2016) 014906. arXiv:1605.08303, doi:10.1103/PhysRevC.94.014906.